

# Triaxiality in $^{48}\text{Cr}$

Andrius Juodagalvis<sup>1</sup>, Ingemar Ragnarsson and Sven Åberg

Div. of Mathematical Physics, Lund Institute of Technology, P.O. Box 118, S-221 00 Lund, Sweden

September 30, 1999

(Submitted to *Phys.Lett.B*)

**Abstract:** Rotational behavior inducing triaxiality is discussed for  $^{48}\text{Cr}$  in the cranked Nilsson-Strutinsky (CNS) model, as well as in the spherical shell model. It is shown that the low-spin region up to about  $I=8$ , has a prolate well-deformed shape. At higher spins the shape is triaxial with a “negative- $\gamma$ ” deformation, that is, with rotation around the classically forbidden intermediate axis. By comparing calculated  $B(E2)$ -values and spectroscopic quadrupole moments in the CNS with spherical shell model results and experimental data, the triaxial rotation around the intermediate axis is confirmed.

*PACS:* 21.10.G; 21.10.Ky; 21.60.C; 21.60.Cs; 21.60.Ev; 23.20.-g; 27.40.+z

*Keywords:* Nuclear structure; shell model; collective model; cranked Nilsson-Strutinsky; calculated electromagnetic moments and transitions; nuclear deformation; yrast states; triaxiality; quantum fluctuations;  $^{48}\text{Cr}$ .

Quantum triaxiality is a most interesting topic in nuclear structure physics. Although the possibility to obtain nuclear shapes with all three axes unequal has been discussed for many years (see e.g. ref. [1]), many unanswered questions exist. For example, the predicted wobbling mode [2, 3] has not yet been observed in any nucleus (although preliminary experimental information [4] may indicate the existence of a wobbling band in  $^{163}\text{Lu}$ ). In classical mechanics rotation around the axis with the middle moment of inertia is forbidden. In the (one-dimensional) cranking approach this would correspond to “negative- $\gamma$ ” rotation (in the Lund convention on  $\gamma$  [3]), and it is still an open question if such a coupling between the intrinsic axes and the rotational axis is realized. Electromagnetic properties, such as quadrupole transitional ( $\Delta I=2$  and 1) and spectroscopic moments, as well as  $M1$  and  $g$ -factors, are expected to be strongly dependent on the triaxiality. They also depend on the rotation axis, and may thus serve as good tests of suggested coupling schemes, and on triaxiality [1].

In Ref. [3] it was concluded that particles in high- $j$  shells which are half-filled or close to half-filled tend to polarize the nucleus towards negative  $\gamma$ -values. From this point of view,  $^{48}\text{Cr}$  should be a good candidate for this kind of rotation because both the proton and the neutron configurations correspond to half-filled  $f_{7/2}$ -shells.

The nucleus  $^{48}\text{Cr}$  is well studied experimentally [5], as well as in extensive shell model calculations [6, 7]. By comparing mean field cranked Nilsson-Strutinsky (CNS) calcula-

---

<sup>1</sup> Tel: +46-46-222 9087, fax: +46-46-222 4416, e-mail: AndriusJ@MatFys.LTH.se

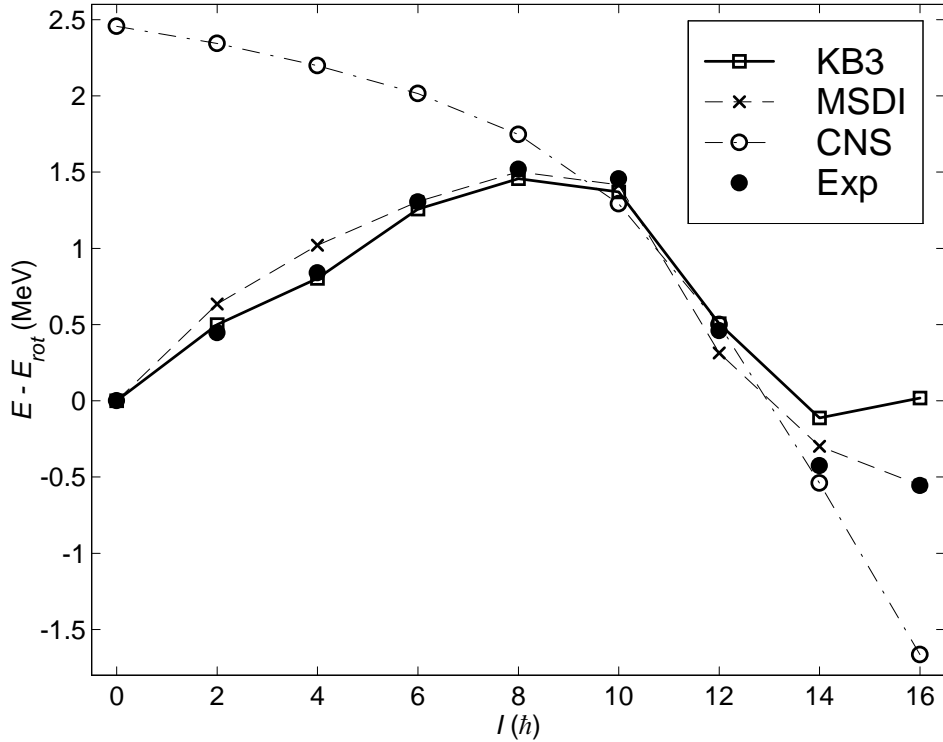


Figure 1: Calculated and measured energies for yrast states in  $^{48}\text{Cr}$ . The solid line shows values calculated in the shell model with the KB3-interaction [7] (model space is full  $fp$  shell), and the dashed line shows shell model results obtained with the modified surface-delta interaction, MSDI [8] (model space is  $f_{7/2}p_{3/2}$ ). The dot-dashed line shows the calculated energies in the cranked Nilsson-Strutinsky model without pairing, CNS. Measured energies are shown by filled circles [5]. A rotational reference,  $E_{rot}=0.051 I(I+1)$ , has been subtracted.

tions with full  $fp$ -shell model calculations, conclusions can be drawn about the rotational behavior as a function of angular momentum. From calculated  $B(E2)$  values and spectroscopic quadrupole moments we find that  $^{48}\text{Cr}$  indeed becomes triaxial at higher spins, with rotation around the intermediate axis (“negative- $\gamma$  rotation”).

Measured and calculated energies of the ground-state band of  $^{48}\text{Cr}$  are shown in fig. 1. For convenience a rotational reference has been subtracted. It is seen how the rotational behavior, the backbending and band termination, are all very well described by the shell model calculations, while the CNS calculation is not able to describe neither the low-spin regime nor the transition energy of the terminating  $16^+$  state. In the CNS calculations, the configuration-constrained approach described in Refs. [9, 10] is used with standard single-particle parameters [9] for the Nilsson potential. In the ground-state, the 8 valence particles occupy the (deformed)  $f_{7/2}$  shell. This corresponds to positive parity and signature 0 (even spins), and gives lowest energy for all states up to  $16^+$ . We allow for a free minimization in the two quadrupole degrees of freedom,  $\varepsilon$  and  $\gamma$ , as well as in one hexadecapole degree of freedom,  $\varepsilon_4$ . The discrepancy between calculation and experiment at low spins is expected since no pairing is included in the CNS calculation. The underestimation by about 1 MeV in the description of the band terminating state at  $I^\pi=16^+$ , indicates that pairing (mainly proton-neutron  $T=1$  pairing [8]) plays an important role

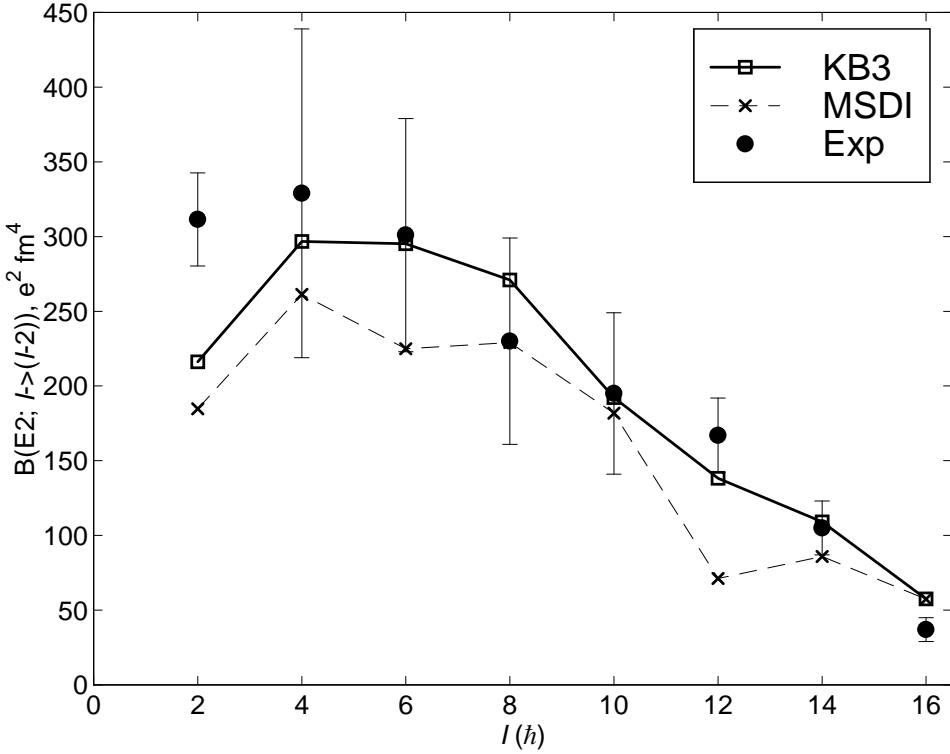


Figure 2: Calculated and measured  $B(E2)$ -values for yrast states in  $^{48}\text{Cr}$ . The solid line shows values calculated in the shell model (full  $fp$ -shell) using the KB3-interaction [7], and the dashed line shows calculated results in the restricted model space ( $f_{7/2}p_{3/2}$ ) using the modified surface-delta interaction, MSDI (cf. [8]). Measured  $B(E2)$ -values [5, 14] are shown with error bars.

also at quite high spin states.

The shell model results show the outcome of two calculations, one performed in the full  $fp$  shell with the KB3 interaction (cf. [7]), and another performed in the restricted subspace  $f_{7/2}p_{3/2}$  with the modified surface-delta interaction, MSDI (cf. [8]). When calculating electromagnetic properties, in both cases standard effective charges  $q_\pi=1.5e$  and  $q_\nu=0.5e$  were used. The calculations were performed using code ANTOINE [11]. Notice that the shell model calculation in the restricted subspace  $f_{7/2}p_{3/2}$  (“quasi-SU(3)” [12]) describes the energies equally well as the full  $fp$  shell calculation. The distribution of shell occupancy in  $f_{7/2}$  is actually quite similar, not only in the two shell model calculations, but also in the CNS calculation [13], as well as in CHFB [6], in spite of the fact that the energies are poorly described in the latter models. This is a result of the quadrupole deformation, that simulates the shell mixing very well [12]. It is then interesting to study the properties that are specifically dependent on the quadrupole degree of freedom, i.e.  $E2$  transition probabilities and spectroscopic quadrupole moments.

In fig.2 we show calculated and experimental  $B(E2)$  values for stretched quadrupole transitions along the ground-state band in  $^{48}\text{Cr}$ . It is seen that the calculated values in the full  $fp$  shell (KB3 interaction), as well as in the restricted  $f_{7/2}p_{3/2}$  subspace (MSDI interaction) come close to the measured  $B(E2)$  values. Since the full  $fp$  shell calculation agrees somewhat better with the data we shall prefer this model in later comparisons. However, the same conclusions can be drawn from the MSDI calculation.

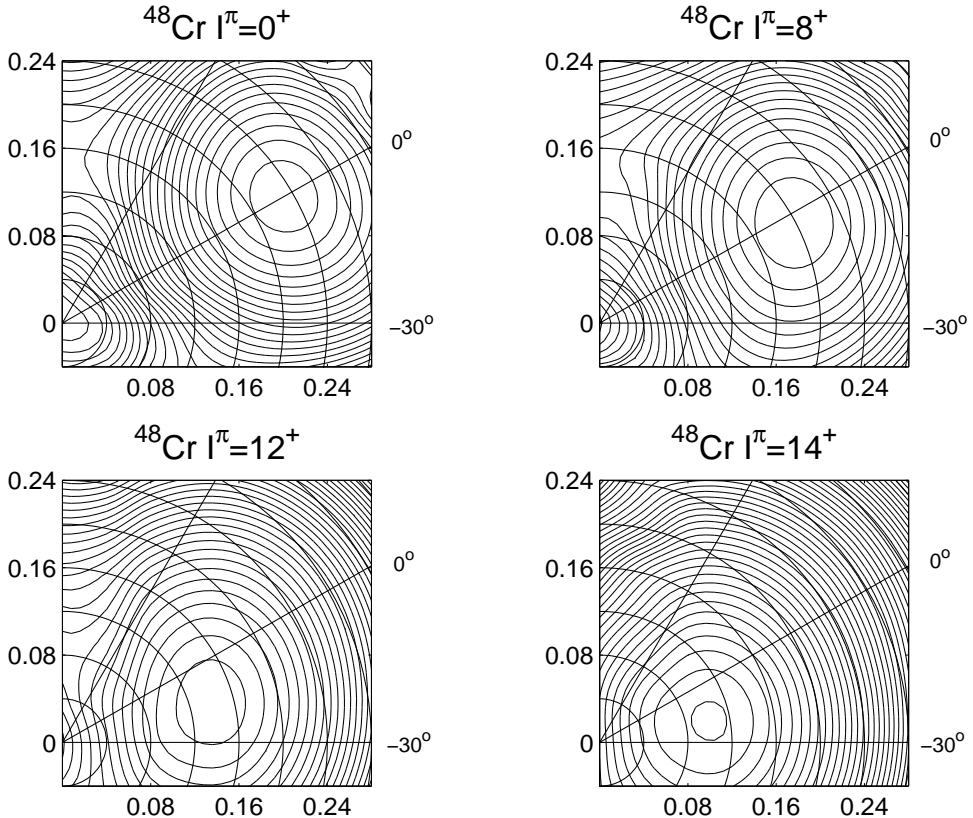


Figure 3: Calculated potential-energy surfaces in the CNS model for  $^{48}\text{Cr}$  at  $I^\pi=0^+$ ,  $8^+$ ,  $12^+$ , and  $14^+$ . The line  $\gamma=0^\circ$  corresponds to prolate shapes with collective rotation, and  $\gamma=60^\circ$  to oblate shapes and non-collective rotation. The contour line separation is 0.2 MeV.

The energies calculated in the CNS approach are illustrated above (fig.1), and potential-energy surfaces for the states  $0^+$ ,  $8^+$ ,  $12^+$ , and  $14^+$  are shown in fig.3. Resulting equilibrium deformations are shown in fig.4. The deformation of the ground state is found to be prolate with  $\varepsilon \approx 0.26$  with the four protons and four neutrons in the  $f_{7/2}$  shell occupying the deformed orbits having  $\Omega = \pm 1/2$  and  $\pm 3/2$ . The deformation shrinks somewhat as the angular momentum increases, and the  $8^+$  state has  $\varepsilon \approx 0.20$ . With increasing angular momentum the equilibrium deformation clearly becomes triaxial, and e.g. the  $12^+$  state has  $\gamma \approx -15^\circ$ . This corresponds to rotation around the (classically forbidden) intermediate axis. Finally, the  $16^+$  state is constructed by aligning all 4 protons and 4 neutrons in the  $f_{7/2}$  shell in the orbits quantized along the rotation axis (the  $x$ -axis) with  $m_j = +1/2, +3/2, +5/2$  and  $+7/2$ , i.e.  $I = 2 \cdot 8 = 16$ , the maximal angular momentum that can be built within this configuration. Thus, the rotational band terminates at  $16^+$  in an approximately spherically symmetric state. Similar deformations are found in cranked Hartree-Fock-Bogoliubov (CHFB) calculations with the finite range density dependent Gogny force [6], see fig.4.

Now two questions emerge: Does the CNS result for the quadrupole shapes have any physical relevance, in spite of the rather poor description of energies (see fig.1), and if so, can the suggested triaxial behavior with negative  $\gamma$ , be tested? We shall approach the first question in a pragmatic way, namely by calculating measurable properties in the CNS,

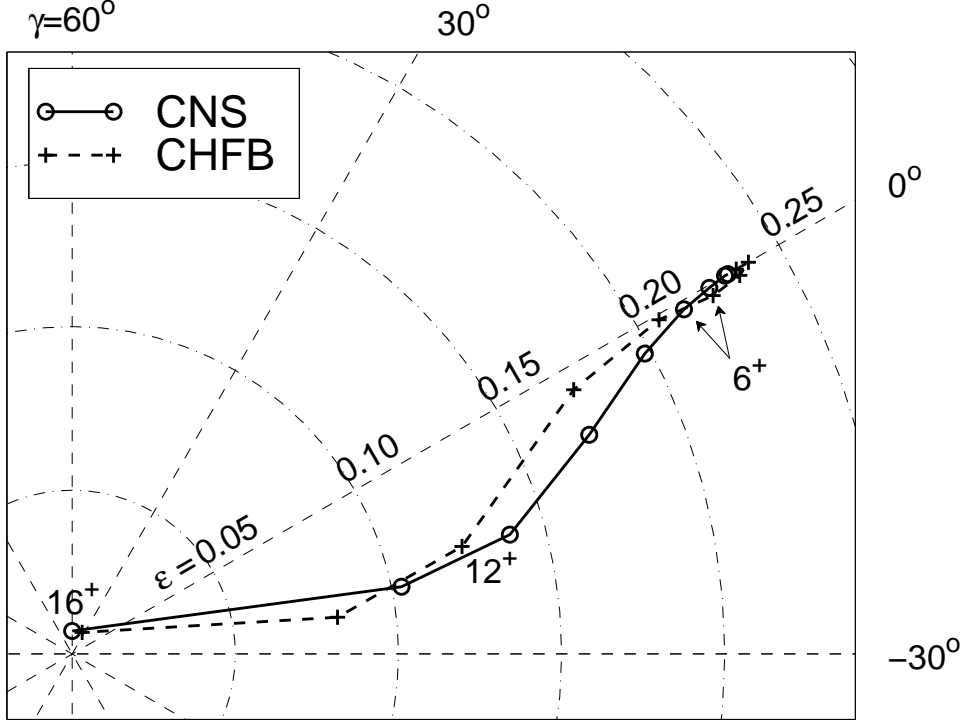


Figure 4: Calculated equilibrium deformations in the  $(\varepsilon, \gamma)$ -plane for the yrast states,  $I^\pi=0^+-16^+$ , in  $^{48}\text{Cr}$ . CNS values are shown by circles, while CHFB results [6] are shown by plus signs. The latter values were obtained transforming  $(\beta, \gamma_\beta)$  to  $(\varepsilon, \gamma)$  under the assumption that the ratio of axes should be preserved.

and compare to shell model results, which agree excellently with (available) experimental data. This comparison will also show the relevance of the calculated triaxiality.

In the rotor model, assuming a fixed (axial) intrinsic electric quadrupole moment of  $Q_0(\hat{z})$ , where  $z$  is the symmetry axis, stretched ( $\Delta I=2$ )  $B(E2)$  values and spectroscopic quadrupole moments  $Q_{spec}$  are calculated as [2, p.45],

$$B(E2; I+2, K \rightarrow I, K) = \frac{5}{16\pi} \langle I+2 | K 20 | I K \rangle^2 Q_0(\hat{z})^2, \quad (1)$$

and

$$Q_{spec} = \langle II 20 | II \rangle \langle I K 20 | I K \rangle Q_0(\hat{z}), \quad (2)$$

respectively. The motion is quantized along the  $z$ -axis, and  $K$  is the angular momentum component along this axis. For triaxial shapes the  $K$  quantum numbers are mixed and the above relations cannot be used. If, however,  $I \gg K$  it is possible to derive similar expressions by instead quantizing the angular momentum along the rotation axis, the  $x$ -axis. For arbitrary triaxial shapes the corresponding expressions become [2, p.193],

$$B(E2; I+2, K_x=I+2 \rightarrow I, K_x=I) = \frac{5}{16\pi} Q_2(\hat{x})^2, \quad (3)$$

and

$$Q_{spec}(I, K_x=I) = Q_0(\hat{x}), \quad (4)$$

where  $Q_2(\hat{x})$  and  $Q_0(\hat{x})$  are the electric quadrupole moments around the rotation axis ( $x$ -axis). The electric quadrupole moments are calculated using the proton wave-functions

at the appropriate equilibrium deformations. In the case of axial symmetry and  $\gamma=0^\circ$ ,  $Q_2(\hat{x})=-\sqrt{3/8}Q_0(\hat{z})$  and  $Q_0(\hat{x})=-(1/2)Q_0(\hat{z})$ , and the expressions in eqs.(3) and (4) coincide with the high-spin limits of the expressions given in eqs.(1) and (2). For the calculated low-spin shapes in  $^{48}\text{Cr}$  (axially symmetric) eqs.(1) and (2) may be applied, and for the higher spins ( $I \gtrsim 10$ ), the expressions (3) and (4) are reasonable approximations. To involve both regions in one smooth expression, we combine the two formulae into,

$$B(E2; I+2, K \rightarrow I, K) = \frac{5}{16\pi} \langle I+2 | K 20 | I K \rangle^2 Q_2(\hat{x})^2 \cdot \frac{8}{3}, \quad (5)$$

and

$$Q_{spec}(I, K) = \langle II 20 | II \rangle \langle IK 20 | IK \rangle Q_0(\hat{x}) \cdot (-2), \quad (6)$$

where the expressions have been divided by the asymptotic values for the Clebsch-Gordon (C-G) coefficients ( $(\sqrt{3/8})^2$ , and  $(-1/2)$ , respectively). These expressions are thus valid *either* at axial-symmetric shapes for any  $I$  and  $K$ , *or* at triaxial shapes for high-spin values ( $I \gg K$ ), when the C-G coefficients have taken their asymptotic values. The expressions are not valid for triaxial shapes at lower spins. In our study we obtain prolate shapes at low spins and triaxial shapes at higher spins, and we shall use the expressions as convenient interpolations between the regions. The  $K$  value in the above formula are then taken from the axial-symmetric limit, i.e.  $K=0$  for the ground band in  $^{48}\text{Cr}$ .

As one additional approximation, we shall neglect the change of deformation between the mother state and daughter state in calculating transitional quadrupole moments, and insert the wave function of the mother state in calculating the  $B(E2)$  values with the above expressions. In the studied cases this gives smaller  $B(E2)$ -values than the alternative method to use wave-functions of daughter states, or states interpolated between mother and daughter states. We believe this approach is reasonable, since the decay of the mother state is connected with a deformation change, that should slow down the transition.

In principle, the shell model contains all types of correlations, corresponding to deformation degrees of freedom (including triaxiality), three-dimensional rotation, quantum fluctuations, etc. We therefore believe that by comparing calculated properties with shell model results, valuable information is obtained about the validity and restriction of the cranking model, including the above simplified expressions for  $B(E2)$ -values and spectroscopic quadrupole moments.

In fig.5 we compare  $B(E2)$  values calculated in the CNS, utilizing eq.(5), with those calculated in the full  $fp$  shell model, for the ground-state band in  $^{48}\text{Cr}$ . The role of deformation changes is clearly seen. If the deformation is kept fixed to its value in the  $0^+$  state, too large  $B(E2)$  values result (short-dashed line in fig.5). If the deformation is allowed to change, but is restricted to axial deformations, quite reasonable  $B(E2)$  values are obtained; the values are in fact similar to those obtained when allowing for full minimization in the  $(\varepsilon, \gamma, \varepsilon_4)$  space. The effect of triaxiality with negative  $\gamma$ -values on  $B(E2)$  values is thus rather small, while if the calculated  $\gamma$ -values are used with opposite signs (positive  $\gamma$ -values), too small  $B(E2)$ -values appear (dot-dashed curve in fig.5).

The CNS constitutes an approximate mean field theory, and quantum fluctuations may affect the results. In order to estimate the role of quantum fluctuations we perform a simple estimate of fluctuations in the  $\varepsilon$  degree of freedom, that should play the dominant role for corrections on the  $B(E2)$ -values. If the equilibrium deformation at a given angular momentum state is  $\varepsilon_0$ , a harmonic approximation of the potential-energy surface around

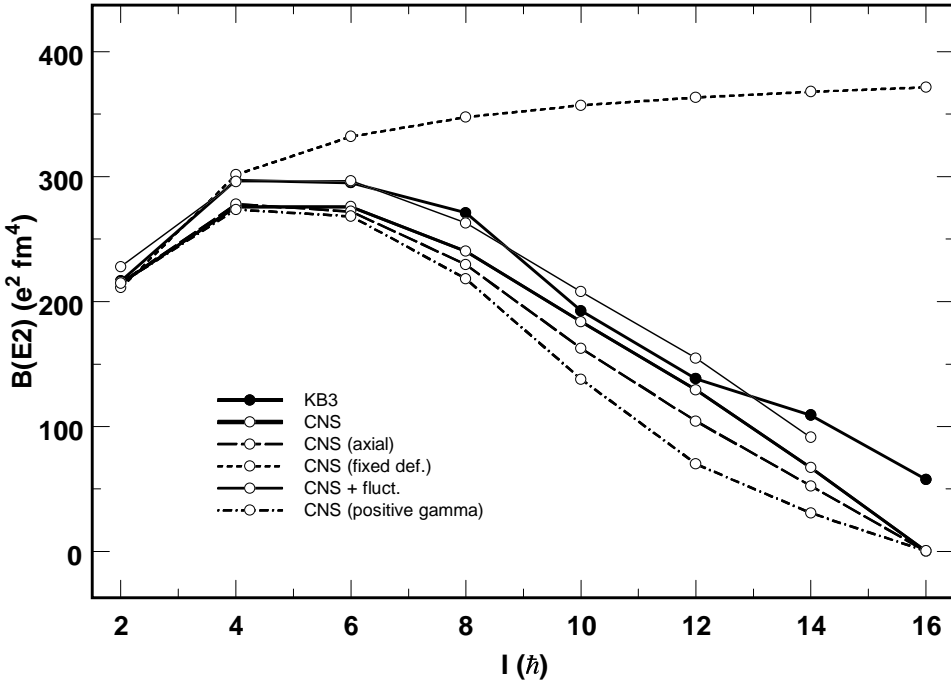


Figure 5: Calculated  $B(E2; I \rightarrow I-2)$ -values for the yrast states of  $^{48}\text{Cr}$ . The curves show the results obtained from the spherical shell model (full  $fp$ -shell) with the KB3 interaction (filled circles connected by thick solid lines) and the CNS (empty circles connected by thick solid lines). The CNS results are also shown assuming constant deformation (empty circles connected by short-dashed lines), deformations restricted to axial shapes (empty circles connected by long-dashed lines), and triaxial shapes with opposite signs on  $\gamma$  (dot-dashed line). Estimates of quantum fluctuations in the  $\varepsilon$ -direction on the full CNS calculations are shown by empty circles connected by thin solid lines.

this minimum yields,

$$E = E_0 + \frac{1}{2}C_\varepsilon(\varepsilon - \varepsilon_0)^2, \quad (7)$$

where the curvature,  $C_\varepsilon$ , is obtained from the calculated potential-energy surfaces at each spin value, see fig.3. The corresponding inertia parameter,  $B_\varepsilon$ , is estimated by [2, p.531]

$$B_\varepsilon = 12B_{irr}. \quad (8)$$

The zero-point motion in the  $\varepsilon$ -direction gives an rms-value of the quadrupole deformation,

$$\varepsilon_{eff} = \sqrt{\varepsilon_0^2 + \varepsilon_{dyn}^2}, \quad (9)$$

where

$$\varepsilon_{dyn} = \frac{1}{2}(B_\varepsilon C_\varepsilon)^{-\frac{1}{2}}. \quad (10)$$

Because the  $B(E2)$  transition probabilities are proportional to  $\varepsilon^2$ , we now estimate the enhancements on  $B(E2)$ -values due to quantum fluctuations in the  $\varepsilon$ -degree of freedom by simply calculating the electric quadrupole moment at the effective deformation,  $\varepsilon_{eff}$ . The results are shown in fig.5 by the thin solid line, and with this estimate of the role of fluctuations the resulting  $B(E2)$ -values are very similar to the shell model results (which include all kinds of fluctuations).

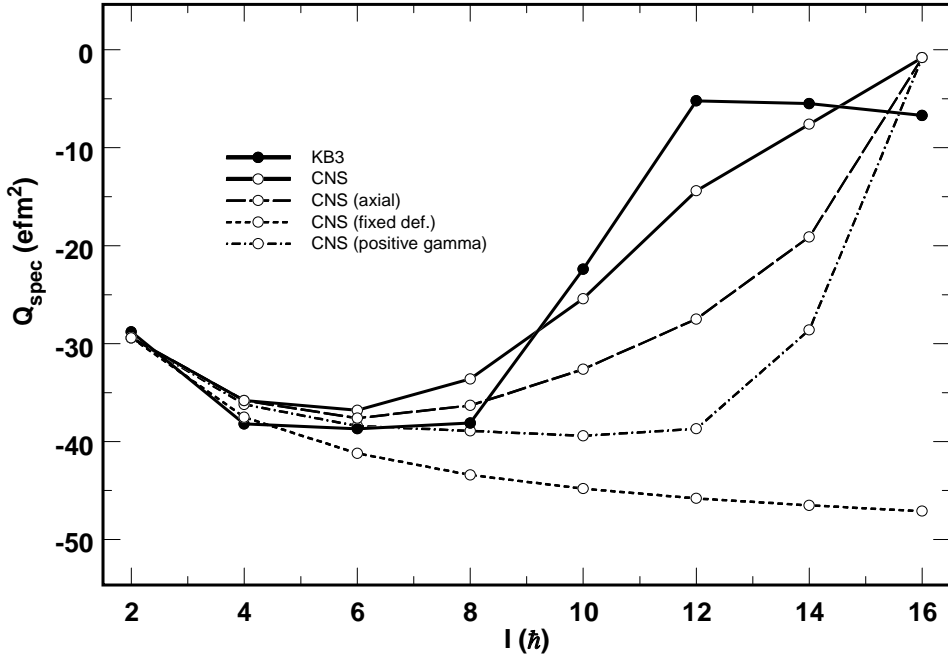


Figure 6: Calculated spectroscopic quadrupole moments for the yrast states of  $^{48}\text{Cr}$ . Lines and symbols have the same meaning as in fig.5

Finally, in fig.6 spectroscopic quadrupole moments are shown. In the same way as for the  $B(E2)$  values the CNS results (calculated from eq.(6)) are shown under four different assumptions, namely deformation fixed to the ground-state value, free deformations but restricted to axial symmetry, free deformations including triaxiality, and calculated triaxial shapes with opposite signs on  $\gamma$  (positive  $\gamma$ -rotation). Also here the importance of deformation changes is clearly seen. If the deformation is fixed to the ground-state shape the spectroscopic moments are completely wrong. However, most interesting is that the spectroscopic moments are indeed a good signature for the proposed rotation scheme, namely that the nucleus obtains a triaxial shape with rotation around the intermediate axis. For example the spectroscopic quadrupole moment of the  $12^+$  state is calculated to be  $-28$  e·fm $^2$  if the shape is restricted to axial symmetry, and  $-14$  e·fm $^2$  if the triaxial shape is considered, that is quite close to the value obtained in the shell model calculation.

For rotation around the intermediate axis quantum fluctuations in the  $\gamma$ -degree of freedom and in the rotational axes (wobbling motion) are expected to be important in determining spectroscopic quadrupole moments [15] (because  $Q_{spec} \propto \varepsilon$ , the fluctuations in  $\varepsilon$  do not contribute to lowest order in this case). The role of these fluctuations were found to be particularly important at low spins and for small  $\gamma$ -values [15] (cf. the discussion above about the validity of eq.(6)). However, in our case the calculated equilibrium  $\gamma$ -deformations, that strongly affect the  $Q_{spec}$ -values, are quite large and appear at substantial spin values. This implies that our main conclusions are expected to remain also if these types of quantum fluctuations are included. Still, it would be of interest to perform a fully dynamical calculation, i.e. to solve the Bohr hamiltonian based on calculated high-spin potential-energy surfaces for  $^{48}\text{Cr}$ .

With triaxial shapes existing over a few spin values a wobbling excitation might principally be possible. We have looked for signatures of such an excitation mode in the shell

model calculations without success. The reason may be that the triaxial deformation is not sufficiently stable and lasts over too few spin values. A more plausible explanation is, however, that the relatively small number of valence particles in  $^{48}\text{Cr}$  only allows for restricted collective phenomena.

In conclusion, we have studied the rotational behavior of  $^{48}\text{Cr}$  and found that the CNS model describes the  $B(E2)$  values as well as spectroscopic quadrupole moments very well, although this model does not include all correlations (such as the pairing interaction) needed for an accurate description of the energy spectrum. The spin states above  $8^+$  are found to be triaxial with rotation around the intermediate axis, and the suggested rotation scheme is confirmed by the spherical shell model calculations. It would be most interesting if these results could be confirmed also by experimental data.

We would like to thank E. Caurier for access to the shell model code [11]. A. J. thanks the Swedish Institute (“The Visby Programme”) for financial support, and I.R. and S.Å. thank the Swedish Natural Science Research Council (NFR).

## References

- [1] I. Hamamoto, Nucl. Phys. **A520** (1990) 297c.
- [2] Aa. Bohr and B.R. Mottelson, Nuclear Structure, vol. II (W.A. Benjamin, New York, 1975).
- [3] G. Andersson et al, Nucl. Phys. **A268** (1976) 205.
- [4] G. Hagemann, private comm.
- [5] F. Brandolini et al, Nucl. Phys. **A642** (1998) 387.
- [6] E. Caurier et al, Phys. Rev. Lett. **75** (1995) 2466.
- [7] E. Caurier et al, Phys. Rev. **C50** (1994) 225.
- [8] A. Juodagalvis and S. Åberg, Phys. Lett. **B428** (1998) 227.
- [9] T. Bengtsson and I. Ragnarsson, Nucl. Phys. **A436** (1985) 14.
- [10] A.V. Afanasjev and I. Ragnarsson, Nucl. Phys. **A591** (1995) 387.
- [11] E. Caurier, computer code ANTOINE, CRN, Strasbourg, 1989.
- [12] A.P. Zuker et al, Phys. Rev. **C52** (1995) R1741.
- [13] A. Juodagalvis and S. Åberg, to be publ.
- [14] T.W. Burrows, Nucl. Data Sheets **68** (1993) 1.
- [15] N. Onishi et al, Nucl. Phys. **A452** (1986) 71.